Polymer Testing 124 (2023) 108104

Contents lists available at ScienceDirect

Polymer Testing

journal homepage: www.elsevier.com/locate/polytest

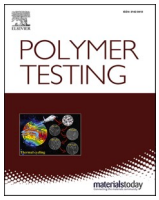

Characterisation of flame retarded recycled PET foams produced by batch foaming

Nóra Lukács [a], Ferenc Ronkay [b], Béla Molnár [c], Botond Marosfői [d], Katalin Bocz [a,*]

[a] Department of Organic Chemistry and Technology, Faculty of Chemical Technology and Biotechnology, Budapest University of Technology and Economics, Műegyetem rkp. 3., H-1111, Budapest, Hungary
[b] Department of Innovative Vehicles and Materials, GAMF Faculty of Engineering and Computer Science, John von Neumann University, 6000, Kecskemét, Hungary
[c] Imsys Ltd, Material Testing Laboratory, Mozaik Street 14/A., H-1033, Budapest, Hungary
[d] Furukawa Electric Institute of Technology Ltd, 1158, Késmárk Street. 28/A., Budapest, Hungary

A B S T R A C T

CO_2-assisted batch foaming was used to manufacture low-density (ρ = 200–350 kg/m^3) microcellular foams from bottle-grade recycled poly(ethylene terephthalate) (rPET) in flame retarded form. The foamability of the PET regrind was enhanced using a reactive chain extender while the flame retardant properties of the rPET foams were improved by incorporating 6% aluminium-tris-(diethylphosphinate) flame retardant (FR). The effects of adding 1% natural montmorillonite (MMT) and polytetrafluoroethylene (PTFE) powder as potential cell nucleating agent and flame retardant synergist were also investigated. As a result of FR addition, the foam structure became less uniform, but the presence of MMT was found to improve uniformity of cellular size and distribution. The applied FR mainly acts in the gas phase as flame inhibitor, but also promotes charring of the foams, as revealed by thermogravimetric analysis (TGA) and pyrolysis combustion flow calorimetry (PCFC). The fine microcellular structure and high cell density allow homogeneous distribution of FR additives, and thus only moderate increase in flammability was observed for the high-porosity (>75%) foams compared to the corresponding bulk materials, as characterized by similar limited oxygen index (LOI) values. In cone calorimeter tests, for the flame retarded foams a 50% reduction in peak heat release rate (PHRR) and a 30% reduction in total heat release (THR) values were measured compared to the FR-free reference. The PTFE addition to the FR formulation was found to increase the time-to-ignition (TTI), reduce PHRR and effective heat of combustion (EHC) while increase charring. The mechanical performance of the flame retarded rPET foams was found to be primarily determined by the apparent density and less affected by the presence of FR additives. Due to strain-induced crystallization occurring during cell growth, the rPET foams are highly crystalline (χ > 25%) which leads to increased thermomechanical resistance compared to unfoamed references.

Author statement

N. Lukács: investigation, visualisation, writing - original draft preparation, F. Ronkay: conceptualisation, methodology, supervision, B. Molnár: investigation, B. Marosfői: methodology, writing - review & editing, K. Bocz: conceptualisation, methodology, writing - original draft preparation, supervision.

1. Introduction

Plastics play an important role in today's society. With plastic packaging materials everyday food waste can be reduced and the shelf-life of products can be increased [1]. In parallel, there is tons of poly (ethylene terephthalate) (PET) waste produced all around the world, causing serious environmental threat since PET is non-biodegradable [2]. Thanks to the improving waste management practices, there is a constantly increasing amount of clean, post-consumer PET raw material which is suitable for mechanical recycling.

The reduction of product weight, thereby reduction of the used raw material can moderate the amount of waste generated. In case of polymers, foaming the raw material can be beneficial, and also adjust new valuable properties to the material [3]. Foaming of polymers can be done by mechanical, physical (PBA – physical blowing agent) or chemical (CBA – chemical blowing agent) methods. As a foaming agent, it is worth choosing a widely available, cheap, non-toxic and low-cost material with favourable properties; that is why CO_2 as a physical foaming agent is becoming more and more popular [4]. When it comes to polymer foaming, not only the choice of foaming agent is a critical issue, but also the technology used can have a great impact on the final cell structure. Basically, batch and continuous technologies can be distinguished. In case of batch processes, the pressure and temperature control are simple, but the diffusion time in the process is much longer than for the extrusion technique, and the time required also depends on the geometry of the specimen [5].

* Corresponding author.
E-mail address: bocz.katalin@vbk.bme.hu (K. Bocz).

https://doi.org/10.1016/j.polymertesting.2023.108104
Received 7 April 2023; Received in revised form 25 May 2023; Accepted 8 June 2023
Available online 9 June 2023

PET foams have the advantage of being resistant to various chemical substances, also being good electrical and thermal insulators [6]. They have relatively high impact and tensile strength and high rigidity. In addition, PET foams are recyclable, making them an environmentally friendly alternative to other polymer foams [7,8]. However, in order to be able to produce foams from recycled PET (rPET), sufficient melt strength is required, as it prevents the cells from collapsing and fusing during cell growth [9,10]. Since recycled PET usually has a lower molecular weight, this is a particular challenge, resulting in an unfavourable morphology and cell structure; the originally linear chain must be modified. The use of chain extenders (CEs) is widespread, increasing the intrinsic viscosity and molecular weight of the material, improving the melt strength, obtaining foams with better structure and mechanical properties [11–13].

As polymer foams are generally considered highly flammable materials due to their porous structure, their flame retardancy is mandatory in many application fields. To reduce ignitability and overall combustion efficiency, flame retardant compounds (FRs) are commonly incorporated during melt processing [14]. In case of PET, FR additives require high thermal stability, and they should not affect the melt strength of the matrix significantly [15]. Since PET has rather poor flame retardant properties, flame inhibition, enhancing char formation, and improving melt dripping behaviour during burning are also necessitated [16].

At first, halogen-containing flame retardant (FR) systems were used for PET products due to their high efficiency, however, due to their environmental damage and toxicity, they have been discarded [17]. In contrast, phosphorus-containing FRs, especially organophosphorus compounds, are well suited for the use in PET-containing systems, since they do not cause smoke, toxicity, or corrosion problems [18–20]. Among the phosphorus-containing compounds, metal phosphinates are the most important flame retardants for PET due to their high phosphorus content, thermal stability and negligible water uptake. The flame retardancy mechanisms of aluminium phosphinate (AlPi) was comprehensively analysed by Schartel and his coworkers in poly(1,4-butylene terephthalate) (PBT) matrix and its glass fibre reinforced composites [21–23]. Accordingly, AlPi plays its main role in the gas phase through flame inhibiton, namely by releasing phosphinate compounds which act as potent free radical scavengers. Besides, catalytic effect of AlPi on charring in the condensed phase was also proposed [24].

To inhibit dripping of melting polymers during combustion, polytetrafluoroethylene (PTFE) is generally used in various systems [25]. In PET matrix, besides effective melt-dripping suppression, PFTE was found to facilitate char formation as well, especially when used in combination with phosphorus-containing FRs [16,26].

In some research, not only FRs, but also nanocomposites were prepared to improve the thermal properties of PET products. Layered silicate materials, such as montmorillonite clay mineral (MMT), are generally used in low concentrations of 1–5 wt% and are known to have char promoting effect during combustion [27]. The effect of MMT addition, however, largely depends on the dispersion quality [28]. Wang et al. [29] prepared a novel FR additive, where MMT was chemically bonded with hexachlorocyclotriphosphazene (HCCP) using (3-aminopropyl)triethoxysilane coupling agent, and used for improving the flame retardancy of PET. With only 3 wt% FR, they managed to achieve UL-94 V-0 classification and an oxygen index of 31.5 vol%. Thermogravimetry was used to test the thermal stability, the residue remaining at 800 °C was 14.7 wt% compared to the initial 6.2 wt%. Ronkay et al. [30] reduced the flammability of rPET with AlPi type FR combined with untreated and organo-modified MMT. V-0 classification was achieved with 4% FR and 1% MMT content. For this composition, time-to-ignition (TTI) during cone calorimeter tests increased by 20–22 s, peak of heat release rate decreased by 25% and noticeable beneficial effect of untreated MMT was revealed on char formation.

Bethke et al. [15] produced foam samples with a density of approximately 200 kg/m^3 from rPET by supercritical carbon dioxide assisted extrusion, with the addition of various FR additives, and the use of pyromellitic dianhydride (PMDA) type CE (0.25–0.40 wt%). Four different phosphorus-containing FRs and one halogen-containing FR were compared; it was found that the halogen-containing system resulted in better processability, however, the phosphorus-containing systems performed better in flammability tests. A 23–31% reduction of PHRR was achieved by using 2–5% phosphorus-based FRs.

Table 1
Composition of the manufactured rPET samples.

Sample	rPET [wt %]	CE [wt %]	FR [wt %]	MMT [wt %]	PTFE [wt %]
rPET/MMT	99.0	–	–	1.0	–
rPET/CE/MMT	98.3	0.7	–	1.0	–
rPET/CE/FR	93.3	0.7	6.0	–	–
rPET/CE/FR/MMT	92.3	0.7	6.0	1.0	–
rPET/CE/FR/PTFE	92.3	0.7	6.0	–	1.0

This AlPi/MMT combination was also utilized to improve the flame retardant properties of microcellular rPET foams manufactured by supercritical carbon dioxide aided extrusion [31]. According to cone calorimeter tests, the additive system provided adequate flame retardancy to the foams, but the reduced LOI values of foamed extrudates indicated noticeably increased flammability of the porous materials compared to the bulk samples of identical compositions.

In this work, flame retarded foams from bottle-grade rPET were manufactured by batch foaming process. The foamability of the PET bottle waste was enhanced using a reactive CE while the FR properties of the rPET foams were improved by incorporating 6% AlPi. Besides, the effects of MMT and PTFE powder as potential cell nucleating agents and FR synergists were investigated [16,32]. The effects of the used additives on the morphology, thermal, flame retardancy and mechanical properties were comprehensively evaluated. Since through batch foaming generally smaller cell size and density is achievable than by foam extrusion [32], the characteristics of the flame retarded rPET foam products obtained via batch process are discussed also in relation to their cellular structure, i.e. in comparison to bulk materials and foam extrudes of previous studies as well.

2. Experimental

2.1. Materials

In this work recycled (rPET) bottle waste with an intrinsic viscosity value (IV) of 0.72 ± 0.02 dL/g was used originating from collected, washed and sorted PET bottles. As a chain extender (CE), Joncryl ADR 4468 (Basf, Germany) a multifunctional epoxy-based styrene-acrylic oligomer was used with a glass transition of 54 °C and molecular mass of 6800 g/mol. For flame retardancy, Exolit OP1240 (Clairant, Switzerland) aluminium-tris-(diethylphosphinate) was used, with a phosphorus content of 23.3–24.0%. Dyneon PTFE TF 1620 (3 M, USA) type poly(tetrafluoro-ethylene) (PTFE) powder (with average particle size of 220 μm) and Cloisite 116 (Byk-Chemie GmbH, Germany) type natural montmorillonite (MMT) were used as co-additives, separately.

2.2. Sample preparation

Flame retardant properties of rPET were improved by incorporating 6% aluminium-tris-(diethylphosphinate) (AlPi) type flame retardant (FR). Based on our previous study [31], 8% of AlPi by itself does not suffice to reach V-0 rating according to the UL94 flammability standard in rPET matrix. However, by using natural montmorillonite (MMT) as synergist, the FR effectivity can be noticeably improved, and V-0 rating becomes achievable at 4% AlPi + 1% MMT content. In this research work, the effects of adding 1% MMT and polytetrafluoroethylene (PTFE) powder as potential flame retardant synergists, when combined with

AlPi, were investigated in rPET bulk and foam materials. Before processing, rPET flakes were dried at 160 °C for 4 h in all cases. After that, they were compounded by LTE 24–44 (Labtech Engineering, Thailand) type twin-screw extruder with zone temperatures between 245 and 260 °C. The exact composition of each sample prepared for optimization of composition is seen in Table 1.

These granules were dried again at 160 °C and then injection moulded into a plaque shape of 60 × 60 × 1 mm^3 dimension with a die temperature of 275 °C and a mould temperature of 60 °C. The melt batch foaming process on these specimens was performed in a high-pressure vessel with carbon-dioxide (CO_2) as physical blowing agent. Firstly, these plaques were put into the high-pressure vessel with the diameter of 8 cm under 60 bar pressure for 48 h. After pressure drop, to slow down the out-diffusion of CO_2, samples were put into a freezer (−18 °C) before foaming. Foaming process was carried out between two PTFE coated iron plates (with 10 mm height), at the temperature of 220 °C. The foaming time was set to 90 s in all cases; during that cell formation was taken place. After foaming, the dimensions of the plaque specimens, depending on the composition, varied in the following ranges: width and length: 90.3 ± 9.4 mm, height: 2.5 ± 0.2 mm.

2.3. Characterization of samples

2.3.1. Scanning electron microscopy

The cell morphology of the foamed PET samples was observed using an EVO MA 10 (Zeiss, Germany) scanning electron microscope (SEM). The SEM specimens were coated by golden layer, the accelerating voltage was 15.75 kV and the used magnification was 500 × .

The cell-size distribution was determined based on the SEM micrographs. The mean value and standard deviation of the diameter of the cell cross-sections were determined from 300 to 400 measurements on each sample. From the cell-size distribution, different cell size averages can be defined based on the weighting of the mean [33]:

Two different cell diameter averages were considered, one is the number-weighed mean diameter (d_1), calculated from the sum of the measured diameters divided by the number of measured cells (N):

$$d_1 = \frac{\sum_{i=1}^{N} d_i}{N} \tag{1}$$

The second is the diameter of a sphere having a volume equal to the mean cell volume (d_2) calculated by the following formula:

$$d_2 = \left(\frac{\sum_{i=1}^{N} d_1^3}{N} \right)^{1/3} \tag{2}$$

The polydispersity degree (PD) was defined as the ratio of d_1 and d_2 diameters.

Energy dispersive X-ray spectroscopic (EDS) analyses were conducted using an Octane Pro type (AMATEX EDAX, Mahwah, NJ, USA) apparatus. Elemental mapping was performed to characterize the spatial distribution of phosphorus in the cellular structure of the foam samples by using an accelerating voltage of 15 keV and a magnification of 1000 × .

2.3.2. Density measurement

The mass densities of foamed rPET samples were measured by Archimedes' Buoyancy test method according to ASTM D792-20. The values were obtained by averaging the results of 5 specimens. The expansion ratio was defined as the ratio of densities of the bulk material to that of the foamed material for each composition. The porosity or the so-called void fraction was calculated from the apparent density of foamed (ρ_{foam}) and the bulk (ρ_{bulk}) samples, according to the following equation:

$$V(f) = 100 * \left(1 - \frac{\rho_{foam}}{\rho_{bulk}} \right) \tag{3}$$

Cell density (N_0) is determined as

$$N_0 = \left(\frac{n}{A} \right)^{\frac{3}{2}} \tag{4}$$

where n is the number of cells in the SEM images of area A in cm^2.

2.3.3. Differential scanning calorimetry

The thermal behavior of the PET samples was investigated using a DSC131 EVO (Setaram, France) type differential scanning calorimeter (DSC) under nitrogen atmosphere. The 5–8 mg samples were heated from 30 °C up to 320 °C at a heating rate of 20 °C/min. Crystallinity of each specimen was calculated of the crystallization enthalpy with the equation below:

$$CRF = \frac{\Delta H_m - \Delta H_{cc}}{\Delta H_f \bullet (1 - \alpha)} \bullet 100\ [\%] \tag{5}$$

where CRF is the crystalline fraction [%], ΔH_m is the crystal melting enthalpy [J/g], ΔH_{cc} is the cold crystallization enthalpy [J/g], α is the ratio of additives [−].

2.3.4. Dynamic mechanical analysis (DMA)

Measurements were carried out using TA Instruments Q800 (New Castle, USA) apparatus to determine loss factor and storage modulus in a temperature sweep mode, in a temperature range of 10–140 °C, with a heating rate of 3 °C/min and a frequency of 10 Hz. The nominal length of the specimen was 64 mm, in case of plaques the nominal width was 1 mm. Specimens were loaded in a dual cantilever configuration.

2.3.5. Thermogravimetric analysis (TGA)

Thermogravimetric measurements were performed using TA Q5000 (New Castle, USA) type instrument in a temperature range of 35–800 °C with a heating rate of 10 °C/min and nitrogen gas flow of 25 ml/min. The mass of the samples was between 5 and 8 mg, tests were repeated three times on each sample.

2.3.6. Pyrolysis combustion flow calorimetry (PCFC)

Pyrolysis combustion flow calorimetric measurements were performed on Fire Testing Technology FAA Micro Calorimeter (FTT, United Kingdom) type instrument according to method A described in the ASTM D7309 (anaerobic pyrolysis and complete combustion). The applied heating rate was 1 °C/min, the maximum pyrolysis temperature in nitrogen atmosphere was 750 °C and the combustion temperature in an excess of oxygen was 900 °C. About 4–5 mg of sample was used in each test and the oxygen to nitrogen volume fraction in the combustor was approximately 20–80. Three parallel measurements were done for each foamed sample.

2.3.7. Limiting Oxygen Index (LOI)

Limiting Oxygen Index (LOI) value represents the lowest oxygen to nitrogen volume ratio in which the burning of the sample is still self-supporting. LOI measurements were carried out according to ASTM D 2863 standard using a Fire Testing Technology (FTT, United Kingdom) instrument. The specimen dimensions for the injection moulded bulk samples were 60 × 10 × 1 mm^3, while for the foamed samples rectangular specimens of 10 ± 0.1 mm width, 90.3 ± 9.4 mm length and thickness ranging between 2.1 and 2.7 mm, depending on the composition, were tested. The LOI results are reproducible to an accuracy of ±0.5%.

2.3.8. UL-94 flammability test

The UL-94 flammability testing ranks the samples according to their ease of ignition, flame spreading rate and production of flammable

Table 2
Density values, expansion ratio and porosity of bulk and foamed rPET samples.

Sample	Bulk density [kg/m^3]	Foam density [kg/m^3]	Expansion ratio [−]	Porosity [%]
rPET/MMT	1380	286 ± 3	4.83 ± 0.06	79.3 ± 0.2
rPET/CE/MMT	1378	303 ± 7	4.55 ± 0.11	78.0 ± 0.5
rPET/CE/FR	1367	255 ± 5	5.37 ± 0.11	81.4 ± 0.4
rPET/CE/FR/MMT	1377	332 ± 5	4.15 ± 0.06	75.9 ± 0.5
rPET/CE/FR/PTFE	1376	218 ± 5	6.32 ± 0.15	84.2 ± 0.4

drippings. Standard UL-94 flammability tests were performed on bulk and foamed samples as well. The specimen dimensions for the injection moulded bulk samples were 60 × 10 × 1 mm^3, while for the foamed samples rectangular specimens of 10 ± 0.1 mm width, 90.3 ± 9.4 mm length and thickness ranging between 2.1 and 2.7 mm, depending on the composition, were tested.

2.3.9. Cone calorimetry

Cone calorimetry tests were carried out using TCC 918 (Netzsch, Germany) type instrument. Two pieces of foamed rPET plates were placed on top of each other, thus samples with weights of 12.0 ± 1.3 g were tested while sample thicknesses varied in the range of 4.2–5.4 mm. The samples were exposed to a constant heat flux of 35 kW/m^2. Heat release values were recorded in the function of time of which the heat release rate (HRR), the peak value of the heat release rate (pHRR) and the total heat release (THR) were evaluated. Average effective heat of combustion (EHC [MJ/kg s]) was computed from the THR divided by the total mass loss (TML). From the measured data, Flame Retardancy Index (FRI) [34] was also calculated according to the following equation:

$$FRI = \frac{\left[THR * \left(\frac{pHRR}{TTI}\right)\right]_{reference\ polymer}}{\left[THR * \left(\frac{pHRR}{TTI}\right)\right]_{FR\ Composite}}$$

All samples were tested in duplicate. The error range of the calculated results was in the case PHRR lower than 15%, in the case of TTI and residual mass lower than 10%, and in the case of THR lower than 5% in all cases.

2.3.10. Three-point-bending

Mechanical properties of PET samples were investigated using 3369 (Instron, USA) type universal mechanical instrument at room temperature. Initial test speed was 2 mm/min and 10 mm/min, support span was 62 mm.

3. Results and discussion

Injection moulded rPET plates with compositions according to Table 1 were subjected to batch foaming procedure to obtain low-density foam products. Composition-structure-property relationships were explored using morphological, thermal, flammability and mechanical test methods.

3.1. Morphology of rPET foams

To determine the expansion ratio and porosity of the samples after batch foaming density measurements were done. Results are shown in Table 2. The nominal density value of each bulk specimen was calculated based on the composition. It can be seen that there is no significant difference between the theoretical bulk densities of the different samples, so in case of the expansion ratio, foam density will be weighty. It was concluded that batch foaming is a suitable method to manufacture flame retarded rPET foam products with significantly reduced density, in the range of 200–300 kg/m^3. Although Bethke et al. [15] were able to manufacture flame retarded rPET foams with density around 100 kg/m^3 by reacting foam extrusion process, the subsequent calibration process resulted in a significant drift of the density falling in a similar range (157–401 kg/m^3 among the different samples) as the present batch foamed products. As it can be seen in Table 2, porosity values of the batch foamed samples are in the range of 75–85% in all cases. Apparently, the additives at the used concentration did not affect noticeably the expansion ability of the composites. In a previous work, Bocz et al. [11] prepared flame retarded rPET foams by supercritical CO_2-assisted extrusion. These rPET foams which contain similar type of additives (CE, MMT and AlPi type FR at 4–8%) have a porosity of 65–80% and are in the same density range as the foams prepared in the current study. From this aspect, the two foaming technologies can result in similar weight reduction.

SEM micrographs were taken from each foam sample with the aim to examine the morphology, cell size and cell-size distribution. As it can be seen in Fig. 1, rather small average cell size of 1–5 μm is characteristic for the rPET/MMT foam (Fig. 1 a). The addition of CE resulted in the increase of the average cell size (15–20 μm) and noticeably increased homogeneity as well (Fig. 1 b). Presumably, the cross-links induced by the CE increased the melt-strength, which is effective to suppress cell coalescence and enables a more stable cell growth. As a result of FR addition, the foam structure became less uniform (Fig. 1 c) accompanied with wider cell size distribution which is likely caused by debonding at the filler-matrix interphase and formation of microholes enabling gas

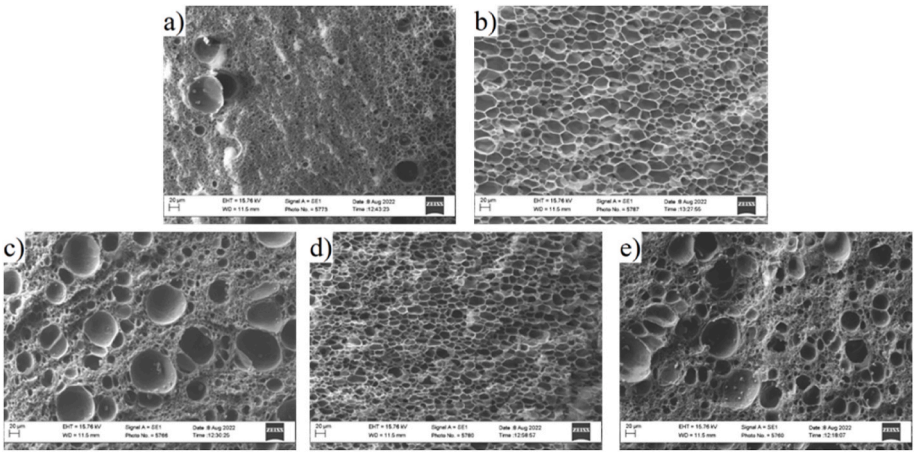

Fig. 1. SEM micrographs of the cross-sections of the foamed rPET samples: a) rPET/MMT, b) rPET/CE/MMT, c) rPET/CE/FR, d) rPET/CE/FR/MMT and e) rPET/CE/FR/PTFE.

Table 3
The number-weighed diameter (d_1); the diameter of a sphere with equal volume to the mean cell volume (d_2) and the polydispersity degree (PD) for each composition.

	Cell density [cells/cm^3]	d_1 mean [μm]	d_2 mean [μm]	PD
rPET/MMT	5.7×10^8	4.2	5.7	1.4
rPET/CE/MMT	3.2×10^7	18.6	21.1	1.1
rPET/CE/FR	1.1×10^8	6.3	16.9	2.7
rPET/CE/FR/MMT	1.4×10^8	13.7	16.6	1.2
rPET/CE/FR/PTFE	1.5×10^8	6.5	12.0	1.9

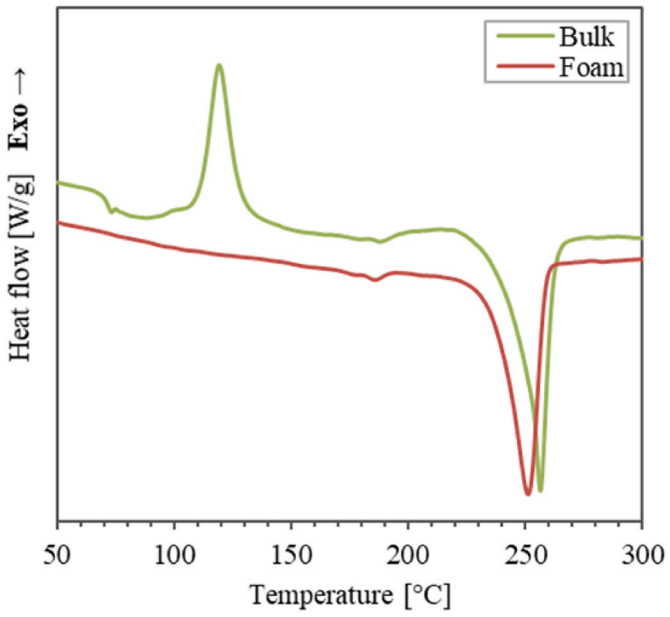

Fig. 2. DSC thermograms of rPET/CE/FR/PTFE bulk and foamed samples.

escape [3]. This is also confirmed by the polydispersity degree (PD) presented in Table 3, inhomogenity increased with the addition of FR; few, but large-volume cells were formed, that considerably influenced the average cell diameter. Nevertheless, in case of the rPET/CE/FR/MMT sample, a uniform, microcellular, closed cellular structure could be achieved (Fig. 1 d). It is proposed that during melt-processing MMT particle may allocate around the surface of the AlPi particles and act as an interfacial adhesion agent [35]. Besides, the effective cell nucleating effect of the nanoclays may contribute to the uniform cell stucture. Similar advantageous effects were not observed for the larger-particle-sized PTFE particles, the morphology of the rPET/CE/FR/PTFE composite (Fig. 1 e) is very similar to that of the rPET/CE/FR foam (Fig. 1 c). Overall, it was concluded that fairly fine cell structures characterized by significantly smaller cell diameters and higher cell density (Table 3) are obtainable by batch procedure (5–20 μm) compared to extrusion foaming (80–500 μm) [31].

3.2. Thermal characterization of rPET samples

For thermal characterization and tracking of structural changes during foaming, DSC analysis was used. In Fig. 2, typical DSC curves can be seen for bulk and foamed samples. Significant cold crystallization and a sharp glass transition temperature can only be observed in case of the bulk rPET samples since rapid cooling during injection moulding resulted in highly amorphous structure. In contrast, due to strain-induced crystallization occurring during cell growth, the foams became highly crystalline, as indicated by the disappearance of the cold crystallization peak in the DSC curve.

Table 4
Glass transition temperature (T_g) and crystalline fraction (CRF) of bulk and foamed rPET samples.

Sample	T_g [°C]		CRF [%]	
	Bulk	Foam	Bulk	Foam
rPET/MMT	72.6	74.1	13.4	29.6
rPET/CE/MMT	72.0	76.9	14.8	28.7
rPET/CE/FR	71.7	77.8	12.7	29.0
rPET/CE/FR/MMT	71.4	77.9	18.3	26.1
rPET/CE/FR/PTFE	71.5	72.6	15.8	26.6

The degree of crystallinity (CRF [%]) obtained from the first heating cycle of the rPET bulk and foam samples are shown in Table 4. It can be seen that the foamed composites have significantly (by 8–16%) higher crystalline fraction than the corresponding bulk samples. During the foaming process performed over the glass transition temperature crystallization is promoted by the chain orientation occurring during cell growth [36]. The increased crystallinity can lead to favourable features such as increased stiffness and heat resistance. The presence of additives did not have a clear effect on the crystallization properties of the composites.

Glass transition temperatures (Tg [°C]) derived from DSC thermograms are also presented in Table 4. As it can be seen, foamed samples have a T_g 2–6 °C higher than the injection moulded plates of the same composition. The higher T_g values of the foams are associated with their higher crystalline ratio. Nevertheless, the measured T_g values seem to be independent from CE or FR content in both (bulk or foam) cases.

Thermo-mechanical response of the rPET samples was investigated by DMA. Typical storage modulus and loss factor curves of rPET composite (rPET/CE/FR/PTFE) before (bulk) and after foaming (foam) are compared in Fig. 3 a and b, respectively. The storage modulus curve of the bulk material starts to decrease sharply at 65 °C, while the corresponding foamed sample begins to lose its resistance to deformation only around 90 °C and less steeply. It was found that the glass transition temperature of the injection moulded rPET samples indicated by the maximum of the loss factor will be approximately 30 °C higher after foaming. These observations are in accordance with the DSC results (Table 4), and suggest that the prepared rPET foams, due to their highly crystalline structure, could have higher service temperature [6].

Fig. 4 presents the TGA curves of the foamed samples. It can be concluded, that although the shapes of the curves are similar, compositions without the FR additive had less residual mass and the decomposition started at lower temperature range.

Characteristic parameters of TGA of rPET compounds before and after foaming are compared in Table 5. Generally, the decomposition temperature (T_{onset}) and the maximum weight loss rate became slightly lower after foaming, and also, in contrast with the bulk samples, the foams had smaller residual mass. Smaller residual mass of foams can be explained based on a previous work of Vadas et al. [3] in which they found that FR particles have inhomogeneous distribution among the cells. As the thin cell walls are poor on FR additives, the charring effect cannot prevail here. The AlPi type FR promoted the charring of the rPET composites as more than 21% charred residue was obtained for both the bulk and foamed FR containing samples. The addition of PTFE resulted in further increase of the residue mass, indicating beneficial solid-phase interaction of PTFE with the AlPi type FR. In case of MMT, this effect is negligible.

3.3. Flame retardant properties of the rPET samples

Flammability of the rPET samples was assessed using pyrolysis combustion flow calorimetry (PCFC), UL-94 tests and limited oxygen index (LOI) measurements, while burning behaviour was investigated using cone calorimetry.

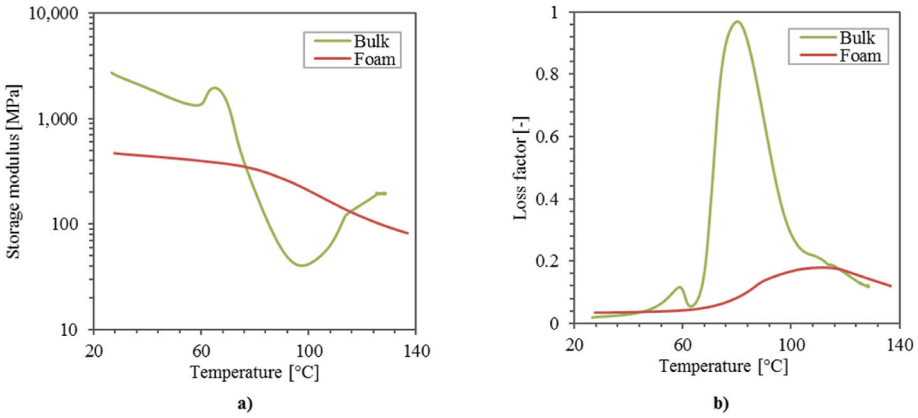

Fig. 3. Comparison of a) storage modulus and b) loss factor of bulk and foamed samples of rPET/CE/FR/PTFE.

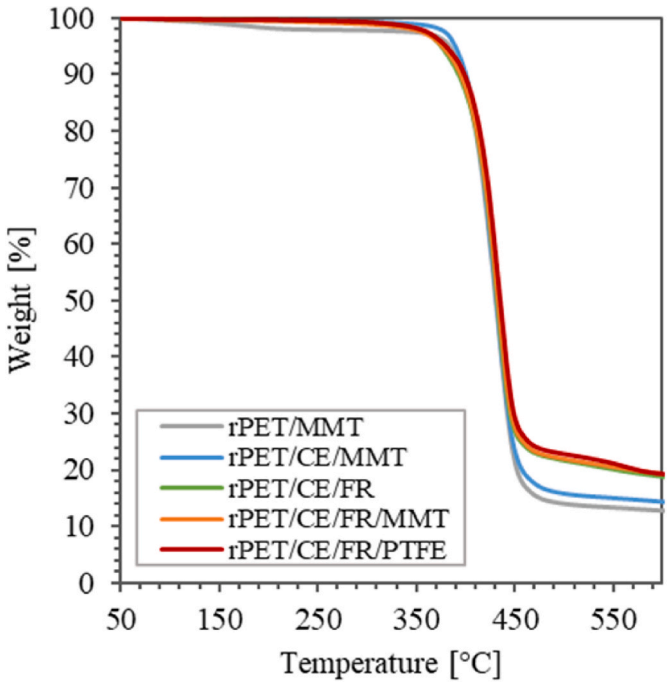

Fig. 4. Thermogravimetric curves of foamed rPET samples with different compositions in N_2 atmosphere.

Table 5
TGA characteristics of different bulk and foamed rPET samples.

Sample	Type	T_{onset} [°C]	T_{max} [°C]	Maximum weight loss rate [%/°C]	Residual mass at 500 °C [%]
rPET/MMT	Bulk	404	434	1.83	14.9
	Foam	404	433	1.77	14.0
rPET/CE/MMT	Bulk	408	438	1.81	16.7
	Foam	404	433	1.83	15.8
rPET/CE/FR	Bulk	408	432	1.89	22.0
	Foam	406	431	1.88	21.7
rPET/CE/FR/MMT	Bulk	410	437	1.83	22.7
	Foam	405	432	1.74	22.0
rPET/CE/FR/PTFE	Bulk	414	436	1.85	23.4
	Foam	407	434	1.74	22.8

Table 6
Pyrolysis combustion flow calorimetry (PCFC) results: peak heat release rate (PHRR), peak temperature (T_p), total heat release (THR) and residual mass values of foamed rPET materials.

Sample	PHRR [W/g]	T_p [°C]	THR [kJ/g]	Residual mass [%]
rPET/MMT	427 ± 7	453 ± 1	16.8 ± 0.2	10.9 ± 0.4
rPET/CE/MMT	401 ± 1	452 ± 1	17.1 ± 0.2	10.9 ± 0.6
rPET/CE/FR	358 ± 15	454 ± 2	15.0 ± 0.6	16.5 ± 0.7
rPET/CE/FR/MMT	379 ± 9	453 ± 1	15.5 ± 0.2	16.3 ± 0.7
rPET/CE/FR/PTFE	356 ± 9	454 ± 1	15.7 ± 0.1	15.0 ± 0.1

Table 7
UL-94 rating and LOI values of different rPET foams and bulk samples.

Sample	UL-94 [rating]		LOI values [vol%]	
	Bulk	Foam	Bulk	Foam
rPET/MMT	V-2	V-2	22.5	22.0
rPET/CE/MMT	V-2	V-2	22.0	21.5
rPET/CE/FR	V-2	V-2	24.5	24.0
rPET/CE/FR/MMT	V-0	V-2	25.5	26.0
rPET/CE/FR/PTFE	V-2	V-2	26.0	25.5

Results of pyrolysis combustion flow calorimetry (PCFC) tests on foamed samples can be seen in Table 6. The addition of AlPi type FR effectively decreased both the peak heat release rate (PHRR) and the total heat release (THR) by 10–15% but there was not significant shifting in peak temperature (T_p) towards one direction. By using 6% AlPi type FR, the residual mass increased from 10.9 to 16.5% indicating condensed-phase activity (charring). Combination of MMT or PTFE with the AlPi type FR entailed a slight increase in THR. Besides, adding MMT moderately increased PHRR, while PTFE addition decreased the residual mass indicating limited contribution of the used co-additives to the condensed-phase activity of the FR formulations. Although PCFC gives some indication about flammability of materials, it is not a real fire test such as cone calorimeter. Therefore, the real fire behaviour of the foamed samples was also investigated under the conditions of a cone calorimeter test.

The results of standard UL-94 flammability tests of bulk and foamed rPET samples are shown in Table 7. Excepting the flame retarded rPET with MMT content that achieved V-0 rating (rPET/CE/FR/MMT), all other samples ignited the cotton wool placed below the vertically mounted specimen and are therefore classified as V-2. The V-0 rating of the rPET/CE/FR/MMT composite is in accordance with the previous studies and confirms that natural MMT forms a synergistic combination

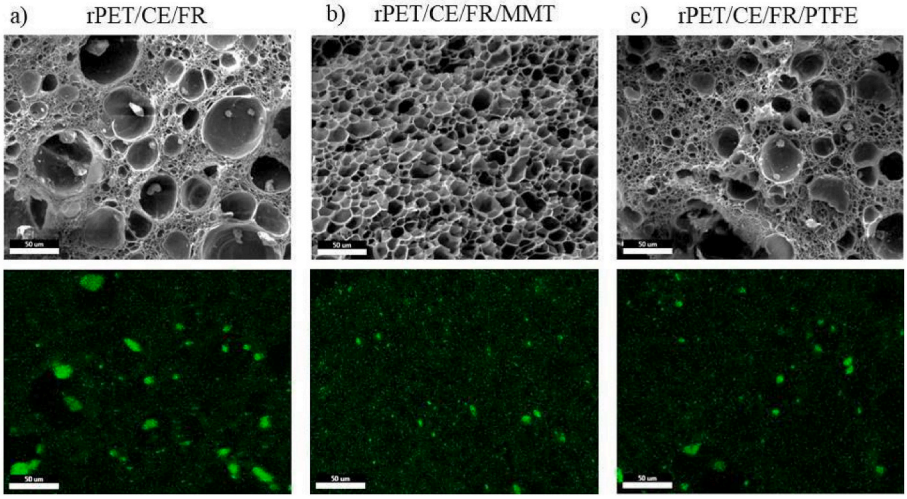

Fig. 5. SEM micrographs and corresponding EDS mapping images of elemental P in a) rPET/CE/FR, b) rPET/CE/FR/MMT, and c) rPET/CE/FR/PTFE foam samples.

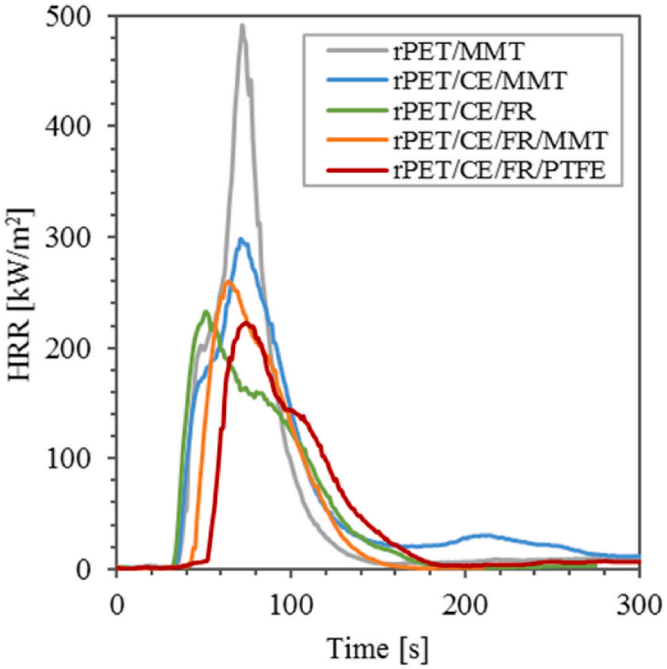

Fig. 6. Heat release rate curves of foamed rPET samples.

with the AlPi type FR [27,30,37]. In case of the foam samples, flaming dipping was characteristic for each test specimens and therefore they are all V-2 rated.

It can be seen in Table 7 that the addition of 6% FR increased the LOI from 22 to 24 vol%. Combination of the AlPi type FR with 1% of MMT or PTFE particles resulted in further increase of the LOI reaching the value of 26 vol%. Considering the uncertainty of LOI measurement of ±0.5%, no significant difference can be established between the LOI values of the injection moulded plates and the corresponding foams. In our previous study, however, a noticeable decrease of the LOI was evinced for flame retarded rPET composites after foaming by supercritical CO_2 assisted extrusion [31]. As in both research studies the rPET composites have similar chemical composition (0.7% CE + 4–8% AlPi + 1% MMT) and similar porosity range of 70–80%, the difference in the flammability properties can be traced back to morphological differences. Namely, the extrusion foaming results in a cellular structure composed of 100–500 μm cells, while the average cell size obtained by batch foaming is

Table 8
Results of cone calorimetry tests of foamed rPET samples.

Sample	TTI [s]	PHRR [kW/m^2]	t(PHRR) [s]	THR [MJ/m^2]	Residue [%]	EHC [MJ/m^{2}g]	FRI [−]
rPET/MMT	34	492	72	18.4	12.6	2.33	1.0
rPET/CE/MMT	34	298	71	20.3	12.3	2.11	1.5
rPET/CE/FR	32	233	51	14.8	22.0	1.68	2.5
rPET/CE/FR/MMT	41	260	64	13.4	22.2	1.61	3.1
rPET/CE/FR/PTFE	52	223	74	13.6	25.7	1.44	4.6

significantly lower, in the range of 5–20 μm. The noticeably increased flammability of the extruded foams can be mainly explained by the increased contact area between the rPET matrix and air and also to the decreased volume concentration of the used FRs in the expanded foam structures [38]. However, these effects seem to be less pronounced in the foam structures with high cell density (Table 3) and small cell size achieved by batch process. The cell density characteristics were assumed to affect the distribution of the used FR additives and thereby the flame retardant performance. EDS analyses were performed to study the distribution of the FR particles in the cellular structure of the flame retarded foams manufactured by batch procedure. It can be seen in Fig. 5 a, that in the cell structure of the rPET/CE/FR foam sample the FR particles are mainly located in the bigger cells, likely formed as a result of filler-matrix debonding. In the presence of MMT, however, the FR particles are homogeneously distributed in the uniform cellular structure (Fig. 5 b). Based on the elemental map shown in Fig. 5 c, the use of PTFE in the composition had only minor effect on the distribution of the FR particles in the foam structure. Nevertheless, the dispersion of the FR particles in all the prepared flame retarded batch foams is obviously better than obtainable in extruded foams with noticeably higher average cell size. This observation, i.e., the uniform distribution of the FR particles in the foam structure, is believed to be the key to achieving only moderate increase in flammability in the case of high-porosity batch foams compared to foam extrudates.

Cone calorimetry tests were performed to characterize the real-scale

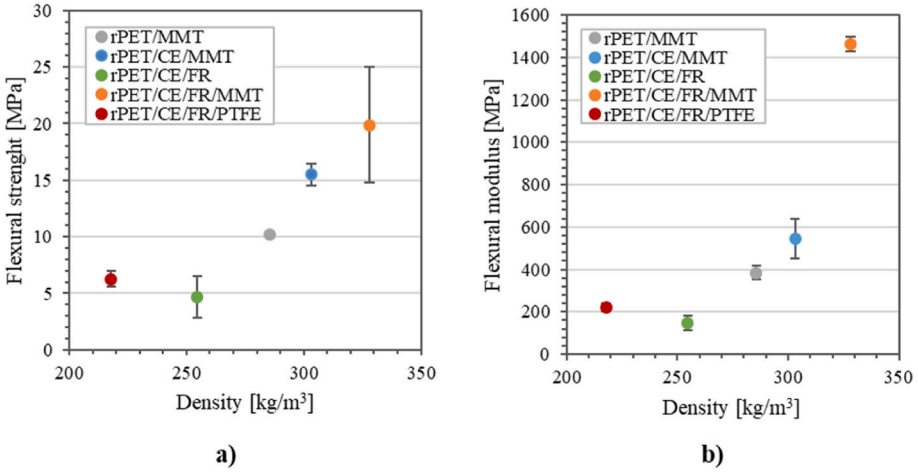

Fig. 7. a) Flexural strength of foamed rPET samples as a function of density and b) Flexural modulus of foamed rPET samples as a function of density.

fire behaviour and flame retardancy performance of the prepared foams. Heat release rate curves are shown in Fig. 6, while combustion characteristics are shown in Table 8. It can be seen that sharp HRR curve with high PHRR value is characteristic for the rPET foam with only 1% MMT content (rPET/MMT). The use of CE resulted in decrease of PHRR but increased THR value. Based on the shape of the HRR curves of the FR-containing foam samples limited charring but intense gas-phase activity can be assumed [39]. EHC values can be used to assess the gas-phase activity, while the amount of residue quantifies the char formation [24]. Based on the significantly reduced PHRR and EHC values corresponding to the rPET/CE/FR sample, flame inhibition is proposed to be the main flame retardant mode of action of the used AlPi type FR. Nevertheless, the presence of AlPi type FR also promoted the charring of the rPET foams as quantified by the increase of the amount of combustion residue (from about 12 to 22%). MMT as co-additive was found to have only negligible effect on char formation. MMT addition resulted in slight reduction of THR but increase of PHRR, without having a noticeable effect on the EHC value. It is assumed that the char promoting effect of the clay is less effective in foam structures than in bulk materials [31], while the catalytic effect of MMT causing acceleration of PET decomposition [40,41] can also occur in foams. The PTFE addition noticeably increased the TTI value and decreased PHRR, THR and EHC as well, and increased the amount of solid residue. Accordingly, char promoting effect can be attributed to the presence of PFTE in the system.

The extent of PHRR reduction (approx. 50%) and THR reduction (approx. 30%) measured for the flame retarded foams compared to the FR-free reference meet the expectations that can be made based on the applied FR formulation [15,30,31]. The cone calorimeter results suggest that the AlPi type FR can be used to improve the flame retardancy properties of rPET foams obtained via batch process as effective as in bulk materials. An FRI of 3.1 was determined for the rPET/CE/FR/MMT foam containing 6% AlPi. This value is also well in line to what is expected based on the composition, since in a previous research study FRI value of 2.0 and 3.9 were obtained for rPET foam extrudates with 4% AlPi+1%MMT and 8%AlPi+1%MMT content, respectively [31]. As it can be seen in Table 8, however, by adding 1% PTFE to 6% AlPi, the FRI of the flame-retarded foams increased noticeably, to a value of 4.6.

3.4. *Mechanical properties of rPET foams*

In order to determine the mechanical behaviour of the rPET foams, three-point bending tests were performed on an Instron universal testing machine. Fig. 7 a and b show the flexural strength and modulus of foamed samples as a function of density, respectively. From these results it can be concluded that the strength and stiffness of the foams are primarily determined by their apparent density. Besides, the skin layer on foams also has a significant contribution to the mechanical performance. Considering the effects of the additives, the addition of the CE improved the flexural properties, but the presence of FR was not favourable.

4. Conclusions

CO_2-assisted batch foaming was found to be a suitable method to manufacture low-denisty ($\rho = 200–350$ kg/m^3) foams from bottle-grade recycled poly(ethylene terephthalate) (rPET) even in flame retarded form. The batch procedure enables the formation of high-porosity (>75%) foams with high cell density and average cell size below 20 μm. In such microcellular structures, homogeneous distribution of FR additives is achievable which is of key importance to show only moderate increase in flammability compared to bulk materials. 6% AlPi proved to be effective in flame inhibition but also promoted charring of the rPET foams; a LOI of 24.0% was reached with this composition. 1% MMT in the formulation was found to act as suitable cell nucleating agent increasing cell uniformity, but synergistic flame retardant effect could not be evinced for this co-additive. PTFE powder at 1% was useful to increase TTI and noticeably reduce PHRR and EHC in cone calorimeter tests, besides increasing the amount of charred residue. For the low-density ($\rho = 220$ kg/m^3) rPET foam with 6% AlPi and 1% PTFE content, a 50% reduction in PHRR and a 30% reduction in THR were achieved compared to the FR-free reference besides reaching a LOI of 25.5%. The mechanical performance of the flame retarded rPET foams, as characterized by three-point bending tests, was found to be primarily determined by the apparent density and less affected by the presence of FR additives. Due to strain-induced crystallization occurring during cell growth, the rPET foams are highly crystalline ($\chi > 25\%$) which leads to favourable features such as increased thermomechanical resistance.

Declaration of competing interest

The authors declare that they have no known competing financial interests or personal relationships that could have appeared to influence the work reported in this paper.

Data availability

Data will be made available on request.

Acknowledgement

The project was funded by the National Research, Development and Innovation Fund of Hungary in the frame of the 2019–1.3.1-KK-2019–00004 and GINOP_PLUSZ-2.1.1-21-2022-00041 projects. The

research was funded by the Hungarian Scientific Research Fund, grant number FK128352. The research was funded by the Sustainable Development and Technologies National Programme of the Hungarian Academy of Sciences (FFT NP FTA). N. Lukács was supported by the ÚNKP-22-2-I-BME-153 New National Excellence Program of the Ministry for Culture and from the source of the National Research, Development and Innovation Fund.

References

[1] C. Matthews, F. Moran, A.K. Jaiswal, A review on European Union's strategy for plastics in a circular economy and its impact on food safety, J. Clean. Prod. 283 (2021), 125263, https://doi.org/10.1016/j.jclepro.2020.125263.
[2] M.M. Ben Zair, F.M. Jakarni, R. Muniandy, S. Hassim, A brief review: application of recycled polyethylene terephthalate in asphalt pavement reinforcement, Sustainability 13 (3) (2021) 1303, https://doi.org/10.3390/su13031303.
[3] D. Vadas, T. Igricz, J. Sarazin, S. Bourbigot, G. Marosi, K. Bocz, Flame retardancy of microcellular poly(lactic acid) foams prepared by supercritical CO2-assisted extrusion, Polym. Degrad. Stabil. 153 (2018) 100–108, https://doi.org/10.1016/j.polymdegradstab.2018.04.021.
[4] Y. Sato, K. Fujiwara, T. Takikawa, S. Sumarno, Takishima, H. Masuoka, Solubilities and diffusion coefficients of carbon dioxide and nitrogen in polypropylene, high-density polyethylene, and polystyrene under high pressures and temperatures, Fluid Phase Equil. 162 (1–2) (1999) 261–276, https://doi.org/10.1016/S0378-3812(99)00217-4.
[5] M. Haurat, M. Dumon, Amorphous polymers' foaming and blends with organic foaming-aid structured additives in supercritical CO2, a way to fabricate porous polymers from macro to nano porosities in batch or continuous processes, Molecules 25 (22) (2020) 5320, https://doi.org/10.3390/molecules25225320.
[6] S. Yao, D. Hu, Z. Xi, T. Liu, Z. Xu, L. Zhao, Effect of crystallization on tensile mechanical properties of PET foam: experiment and model prediction, Polym. Test. 90 (2020), 106649, https://doi.org/10.1016/j.polymertesting.2020.106649.
[7] D.E. Kwon, M.G. Aregay, B.K. Park, Y.-W. Lee, Preparation of polyethylene terephthalate foams at different saturation temperatures using dual methods of supercritical batch foaming, Kor. J. Chem. Eng. 38 (12) (2021) 2560–2566, https://doi.org/10.1007/s11814-021-0889-y.
[8] L. Doyle, I. Weidlich, Hydrolytic degradation of closed cell polyethylene terephthalate foams. The role of the mobile amorphous phase in the ductile-brittle transition, Polym. Degrad. Stabil. 202 (2022), https://doi.org/10.1016/j.polymdegradstab.2022.110022.
[9] L. Di Maio, I. Coccorullo, S. Montesano, L. Incarnato, Chain extension and foaming of recycled PET in extrusion equipment, Macromol. Symp. 228 (1) (2005) 185–200, https://doi.org/10.1002/masy.200551017.
[10] V.A. Szabó, G. Dogossy, Structure and properties of closed-cell foam prepared from rPET, IOP Conf. Ser. Mater. Sci. Eng. 426 (2018), https://doi.org/10.1088/1757-899X/426/1/012043.
[11] K. Bocz, F. Ronkay, B. Molnár, D. Vadas, M. Gyürkés, D. Gere, G. Marosi, T. Czigany, Recycled PET foaming: supercritical carbon dioxide assisted extrusion with real-time quality monitoring, Advanced Industrial and Engineering Polymer Research 4 (3) (2021) 178–186, https://doi.org/10.1016/j.aiepr.2021.03.002.
[12] K. Bocz, B. Molnár, G. Marosi, F. Ronkay, Preparation of low-density microcellular foams from recycled PET modified by solid state polymerization and chain extension, J. Polym. Environ. 27 (2) (2019) 343–351, https://doi.org/10.1007/s10924-018-1351-z.
[13] B. Liu, Q. Xu, Effects of bifunctional chain extender on the crystallinity and thermal stability of PET, J. Mater. Sci. Chem. Eng. 1 (6) (2013) 9–15, https://doi.org/10.4236/msce.2013.16002.
[14] V.A. Szabó, G. Dogossy, Investigation of flame retardant rPET foam, Period. Polytech. - Mech. Eng. 64 (1) (2019) 81–87, https://doi.org/10.3311/PPme.14556.
[15] C. Bethke, D. Goedderz, L. Weber, T. Standau, M. Döring, V. Altstädt, Improving the flame-retardant property of bottle-grade PET foam made by reactive foam extrusion, J. Appl. Polym. Sci. 137 (35) (2020), 49042, https://doi.org/10.1002/app.49042.
[16] X. Zhu, H. Xu, J. Lu, J. Wang, S. Zhou, Effect of fluoropolymer antidripping agent on the microstructure and properties of polyesters, J. Polym. Res. 15 (4) (2008) 295–300, https://doi.org/10.1007/s10965-007-9170-2.
[17] R.A. Mensah, V. Shanmugam, S. Narayanan, J.S. Renner, K. Babu, R.E. Neisiany, M. Försth, G. Sas, O. Das, A review of sustainable and environment-friendly flame retardants used in plastics, Polym. Test. 108 (2022), 107511, https://doi.org/10.1016/j.polymertesting.2022.107511.
[18] D.-M. Ban, Y.-Z. Wang, B. Yang, G.-M. Zhao, A novel non-dripping oligomeric flame retardant for polyethylene terephthalate, Eur. Polym. J. 40 (8) (2004) 1909–1913, https://doi.org/10.1016/j.eurpolymj.2004.03.013.
[19] C. Bascucci, I. Duretek, S. Lehner, C. Holzer, S. Gaan, R. Hufenus, A. Gooneie, Investigating thermomechanical recycling of poly(ethylene terephthalate) containing phosphorus flame retardants, Polym. Degrad. Stabil. 195 (2022), https://doi.org/10.1016/j.polymdegradstab.2021.109783.
[20] C. Zhang, C. Zhang, J. Hu, Z. Jiang, P. Zhu, Flame-retardant and anti-dripping coating for PET fabric with hydroxyl-containing cyclic phosphoramide, Polym. Degrad. Stabil. 192 (2021), https://doi.org/10.1016/j.polymdegradstab.2021.109699.
[21] U. Braun, B. Schartel, Flame retardancy mechanisms of aluminium phosphinate in combination with melamine cyanurate in glass-fibre-reinforced poly(1,4-butylene terephthalate), Macromol. Mater. Eng. 293 (3) (2008) 206–217, https://doi.org/10.1002/mame.200700330.
[22] U. Braun, H. Bahr, H. Sturm, B. Schartel, Flame retardancy mechanisms of metal phosphinates and metal phosphinates in combination with melamine cyanurate in glass-fiber reinforced poly(1,4-butylene terephthalate): the influence of metal cation, Polym. Adv. Technol. 19 (6) (2008) 680–692, https://doi.org/10.1002/pat.1147.
[23] E. Gallo, B. Schartel, U. Braun, P. Russo, D. Acierno, Fire retardant synergisms between nanometric Fe $_2$ O $_3$ and aluminum phosphinate in poly(butylene terephthalate), Polym. Adv. Technol. 22 (12) (2011) 2382–2391, https://doi.org/10.1002/pat.1774.
[24] S. Brehme, T. Köppl, B. Schartel, V. Altstädt, Competition in aluminium phosphinate-based halogen-free flame retardancy of poly(butylene terephthalate) and its glass-fibre composites, E-Polymers 14 (3) (2014) 193–208, https://doi.org/10.1515/epoly-2014-0029.
[25] S. Ebnesajjad, R. Morgan, Polytetrafluoroethylene (PTFE), in: Sina Ebnesajjad, A. Richard, Morgan (Eds.), *Fluoropolymer Additives* (1 St, William Andrew Publishing, 2012, pp. 233–286, https://doi.org/10.1016/B978-1-4377-3461-4.15002-0.
[26] X. Jin, Y. Wang, Z. Zhu, Y. Liu, R. Wang, Effect of combined anti-dripping additive on properties of flame resistant polyester, J. Textil. Res. 39 (8) (2018) 15–21, https://doi.org/10.13475/j.fzxb.20170906407.
[27] L. Ye, J. Ren, S. Cai, Z. Wang, J. Li, Poly(lactic acid) nanocomposites with improved flame retardancy and impact strength by combining of phosphinates and organoclay, Chin. J. Polym. Sci. 34 (6) (2016) 785–796, https://doi.org/10.1007/s10118-016-1799-z.
[28] Y. Wang, J. Gao, Y. Ma, U.S. Agarwal, Study on mechanical properties, thermal stability and crystallization behavior of PET/MMT nanocomposites, Compos. B Eng. 37 (6) (2006) 399–407, https://doi.org/10.1016/j.compositesb.2006.02.014.
[29] J. Wang, Z. Mao, Modified montmorillonite and its application as a flame retardant for polyester, J. Appl. Polym. Sci. 131 (1) (2014), https://doi.org/10.1002/app.39625 n/a-n/a.
[30] F. Ronkay, B. Molnár, F. Szalay, D. Nagy, B. Bodzay, I.E. Sajó, K. Bocz, Development of flame-retarded nanocomposites from recycled PET bottles for the electronics industry, Polymers 11 (2) (2019) 233, https://doi.org/10.3390/polym11020233.
[31] K. Bocz, F. Ronkay, D. Vadas, B. Molnár, D. Gere, T. Czigány, G. Marosi, Flame retardancy of PET foams manufactured from bottle waste, J. Therm. Anal. Calorim. 148 (2) (2023) 217–228, https://doi.org/10.1007/s10973-022-11423-3.
[32] A. Shabani, A. Fathi, S. Erlwein, V. Altstädt, Thermoplastic polyurethane foams: from autoclave batch foaming to bead foam extrusion, J. Cell. Plast. 57 (4) (2021) 391–411, https://doi.org/10.1177/0021955X20912201.
[33] V. Langlois, C.T. Nguyen, F. Detrez, J. Guilleminot, C. Perrot, Permeability of polydisperse solid foams, Phys. Rev. 105 (1) (2022), 015101, https://doi.org/10.1103/PhysRevE.105.015101.
[34] H. Vahabi, B. Kandola, M. Saeb, Flame retardancy index for thermoplastic composites, Polymers 11 (3) (2019) 407, https://doi.org/10.3390/polym11030407.
[35] F. Xin, C. Guo, Y. Chen, H. Zhang, L. Qian, A novel triazine-rich polymer wrapped MMT: synthesis, characterization and its application in flame-retardant poly (butylene terephthalate), RSC Adv. 7 (75) (2017) 47324–47331, https://doi.org/10.1039/C7RA08857D.
[36] T. Standau, C. Zhao, S. Murillo Castellón, C. Bonten, V. Altstädt, Chemical modification and foam processing of polylactide (PLA), Polymers 11 (2) (2019) 306, https://doi.org/10.3390/polym11020306.
[37] A. Ramani, A.E. Dahoe, On the performance and mechanism of brominated and halogen free flame retardants in formulations of glass fibre reinforced poly (butylene terephthalate), Polym. Degrad. Stabil. 104 (2014) 71–86, https://doi.org/10.1016/j.polymdegradstab.2014.03.021.
[38] K. Wang, J. Wang, D. Zhao, W. Zhai, Preparation of microcellular poly(lactiv acid) composites foams with improved flame retardancy, J. Cell. Plast. 53 (1) (2016), https://doi.org/10.1177/0021955X16633644.
[39] B. Schartel, T.R. Hull, Development of fire-retarded materials—interpretation of cone calorimeter data, Fire Mater. 31 (5) (2007) 327–354, https://doi.org/10.1002/fam.949.
[40] A. Leszczyńska, J. Njuguna, K. Pielichowski, J.R. Banerjee, Polymer/montmorillonite nanocomposites with improved thermal properties, Thermochim. Acta 454 (1) (2007) 1–22, https://doi.org/10.1016/j.tca.2006.11.003.
[41] G. Guan, C. Li, D. Zhang, Y. Jin, The effects of metallic derivatives released from montmorillonite on the thermal stability of poly(ethylene terephthalate)/montmorillonite nanocomposites, J. Appl. Polym. Sci. 101 (3) (2006) 1692–1699, https://doi.org/10.1002/app.23318.